Effect of Boron Addition on the Thermal Properties of Diamond-Particle-Dispersed Cu-Matrix Composites Fabricated by SPS

Kiyoshi Mizuuchi[1], Kanryu Inoue[2,3], Yasuyuki Agari[1], Motohiro Tanaka[1], Takashi Takeuchi[1], Jun-ichi Tani[1], Masakazu Kawahara[4], Yukio Makino[5], Mikio Ito[6]

[1]Osaka Municipal Technical Research Institute, Osaka, Japan
[2]Materials Science & Engineering, University of Washington, Seattle, USA
[3]Microbright Corporation, Toyohashi, Japan
[4]Kawahara SPS Technical Office, Yokosuka, Japan
[5]Forum MACKIY, Kyoto, Japan
[6]Center for Atomic and Molecular Technologies, Graduate School of Engineering, Osaka University, Suita, Japan
Email: mizuuchi@omtri.or.jp

Abstract

Diamond particle dispersed copper (Cu) matrix composites were fabricated from the powder mixture composed of diamond, pure-Cu and boron (B) by spark plasma sintering (SPS). The composites were consolidated at 1173 K for 600 s by SPS. The reaction between the diamond particle and the Cu matrix in the composite was not confirmed by SEM observation and X-ray diffraction (XRD) analysis. The relative packing density of the Cu/diamond composites increased with B addition and attained 93.2% - 95.8% at the B content range between 1.8 vol.% and 13.8 vol.%. The thermal conductivity of the diamond-dispersed Cu composite drastically increased with B addition and reached the maximum value of 689 W/mK at 7.2 vol% B. Numerous transgranular fractures of diamond particles were observed on bending fracture surfaces of Cu-B/diamond composites. This indicates strong bonding between the diamond particle and the Cu matrix in the composite. The coefficient of thermal expansion of the composite falls in the upper line of Kerner's model.

Keywords

1. Introduction

Traditional packaging base materials [1] are Cu-W, AlN, BeO and Al/SiC composites

and these all have thermal conductivities, λ, around 200 W/mK. The highest thermal conductivity available in a naturally occurring material is so-called good quality diamond that contains nitrogen less than 85 ppm, and its conductivity is 2000 W/mK [2]. In addition to this property of diamond, it has a low CTE of 2.3 ppm/K [2]. Therefore, diamond powder is considered to be the best candidate as filler particles for heat dissipative materials. Copper (Cu), on the other hand, is also considered to be a good candidate of the matrix material for heat dissipative materials because of its high thermal conductivity (λ = 385 W/mK) [3] and a low price. From these reasons, Cu-matrix composites containing dispersed diamond particles have received wide attention as potential candidates in advanced electronic packaging [4]-[16].

Metal infiltration technique containing belt-type-high pressure technique [17] has been commonly used for the fabrication of particle-dispersed metal-matrix composites because of pore free metal matrix composites (MMCs) that can relatively easily be obtained. When diamond particles are used, however, to make Cu-matrix composites, this technique does not work because of the low wettability of diamond with pure-Cu. Therefore, Weber *et al.* [8], He *et al.* [9] [10], Fan *et al.* [11] and Chen *et al.* [12] fabricated diamond particle dispersed Cu alloy matrix composites by a metal infiltration technique. In these cases, Cu-Cr, Cu-B or Cu-Zr alloy ingots were used in place of a pure-Cu ingot as a matrix material to obtain the strong bonding between diamond particles and Cu matrix. In these cases, however, the process is associated with the carbide formation at the interface between the diamond and Cu during processing. It was reported that the thermal conductivities of 600 - 831.4 W/mK for Cu/50-90vol.% diamond composites [8]-[12]. It should be mentioned, however, that such infiltration processes are involved in processing temperatures higher than the melting point of Cu matrix. This is considered to be a drawback since reductions in thermal conductivity could occur by structural alterations of diamond particles by direct contact with molten Cu. Yoshida *et al.* [5] have reported that the thermal conductivity of diamond drastically decreases when diamond was heated in vacuum for 3.6 ks at a temperature higher than 1223 K.

In order to avoid the above structural alterations, several research works on diamond particle dispersed Cu alloy matrix composites fabricated at temperatures lower than the melting temperature of Cu by vacuum hot pressing (VHP) or spark plasma sintering (SPS) [18]-[29] have been reported by Shubert *et al.* [13] [14], Chu *et al.*, [15] and Mankowski *et al.* [16]. In these cases, atomized Cu-B and Cu-Cr alloy powders were used as matrix materials so as to form carbides at the interface between diamond and Cu. Similar studies were also done by Weber *et al.* [8], He *et al.* [9] [10], Fan *et al.* [11] and Chen *et al.* [12]. The thermal conductivities of 538 - 658 W/mK have been reported for Cu/50-58vol.% diamond composites [13]-[16].

In the present study, in order to avoid the processing temperatures higher than the melting point of Cu as well as the use of high cost Cu alloys that have to specially ordered, the powder mixture of Cu and a third element was prepared as a matrix material. The main purpose of the use of this powder mixture is to try to form strong bonding

between Cu matrix and diamond particles through the formation of carbides at the interface between Cu and diamond via third element particles. We used SPS process to fabricate diamond particle dispersed Cu matrix composites using the B-added Cu matrix powder mixture at a temperature of 1173 K. Microstructures of the composites fabricated are observed by scanning electron microscopy. The bending strengths of the composites are measured for the evaluation of the bonding between diamond particles and Cu matrix in the composite. The packing density and the thermal properties, λ and CTEs, of the composites are measured.
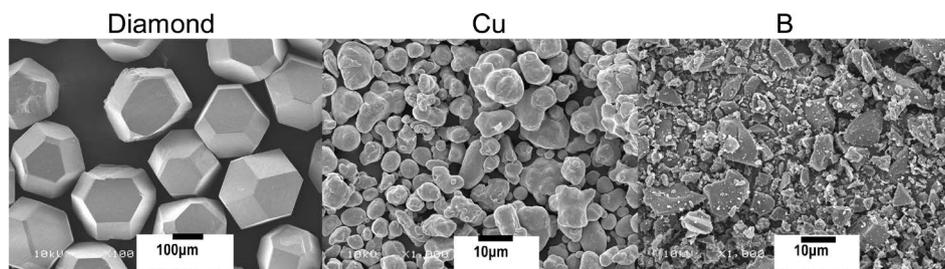
2. Experimental Procedure

In the present study, Ib type synthetic diamond powder (IMS-15, 310 µm, Tomei Diamond Co., Ltd.) was employed as a filler material and its thermal conductivity of the synthetic diamond is estimated to be about 2000 W/mK. As a matrix material, two kinds of metallic powders, pure copper (Cu) powder (Cu-At-W-250, −45 µm, Fukuda Metal Foil & Powder Co., Ltd.) and pure boron (B) powder (BBE01PB, 99% purity, −45 µm, Kojundo Chemical Laboratory Co., Ltd.), were prepared. Scanning electron micrographs of diamond, Cu and B powders used in the present study are shown in **Figure 1**.
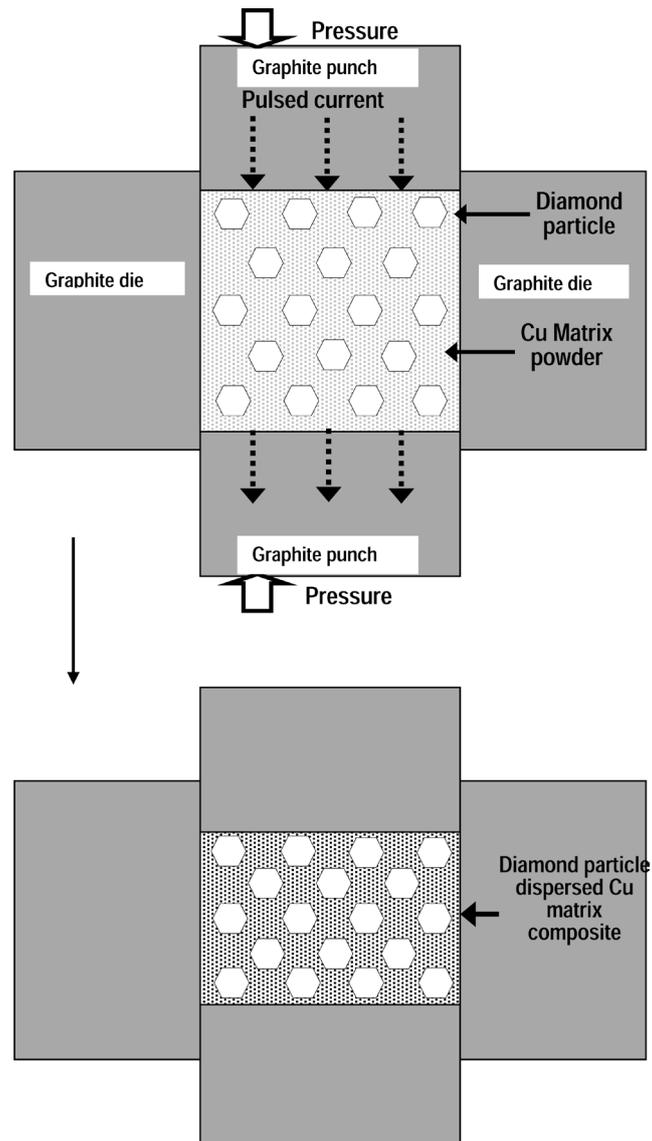
The addition of B powder to Cu powder is important for the improvement of the thermal conductance between diamond and Cu associated with the boron carbide formation at the interface between the diamond particles and the Cu matrix. Thus, in order to obtain the strong bonding between diamond particles and Cu matrix, Cu-based powder mixtures containing various volume fractions (0 - 13.8 vol.%) of B were used as matrix materials in the present study.

Powder mixtures composed of three kinds of powders (diamond, Cu and B powders) were prepared as starting materials, and these powder mixtures with 50 vol.% diamond were processed to fabricate Cu-B matrix composite using an SPS equipment, Model FUJI ELECTRIC DR. SINTER 1020. The equipment consists of an electric power source and a pressure system, and the fabrication of composites is carried out immediately after powder mixtures are placed in a die-set, mostly, made of graphite. A side view of our custom-made cylindrical graphite die-set used in the present study is depicted schematically in **Figure 2** and its details have been described in a previous study [30].

For making one disk-shaped composite specimen with gauge dimensions of 2.5 mm thick and 10 mm in diameter, about 1.2 g of the powder mixture of diamond, Cu and B

Figure 1. SEM micrographs of as-received diamond, Cu and B powders, showing the powder morphology.

Figure 2. Schematic illustration showing processing of diamond particle dispersed Cu-matrix composite by spark plasma sintering (SPS).

was prepared and placed carefully in the above described custom-made die-set, and consolidation was carried out. The gauge dimensions of the graphite die used in the present study are 35 mm outer diameter, 10 mm inner diameter and 40 mm height. During SPS processing, die temperature was monitored by a thermo-couple that was inserted in a hole located in a position 5 mm distant from the inner surface of the die. This thermo-couple hole was drilled on the outside surface of the die with dimensions of 2 mm in diameter and 7.5 mm deep.

The SPS process employed is described in detail as follows. First, the lower punch was inserted into the die from its one end, followed by pouring of 1.2 g of the powder mixture containing diamond particles. Then, the upper punch was placed onto the powder mixture. The powder mixture was pressed at a pressure of 80 MPa through the
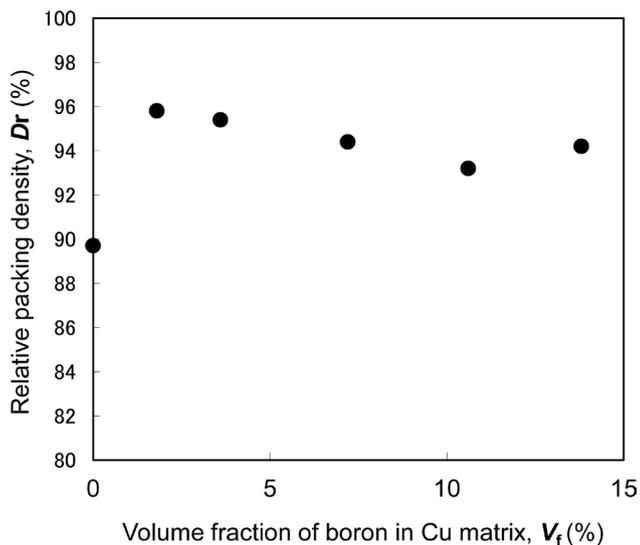
upper and lower punches, and then spark plasma sintering was performed after evacuation to a vacuum of 2 Pa. Sintering was carried out at a temperature of 1173 K at a heating rate of 1.67 K/s. The holding time used was 0.6 ks. To visualize a change in the relative packing density of the diamond-Cu composite during the SPS process, longitudinal displacements between the punches were monitored as a function of time and die temperature. The discharged pulsed current used was about 450 A and sparking was generated at a constant interval of approximately 2.78×10^{-3} s.

Disk-shaped composites fabricated in an above fashion were examined by scanning electron microscopy and X-ray diffraction using a JEOL JSM 6460 LA microscope and RIGAKU Rint-2500 X-ray diffractometer. Diamond-Cu composite disks were gold-coated and their thermal diffusivities were measured by a laser flash technique using an NETZSCH LFA-457 thermal constants analyzer. The achieved packing density of composite disks fabricated was measured by Archimedes method for optimization of process parameters and calculation of thermal conductivities. The bending strengths of the composites measured with INSTRON 5582 testing machine on square-column-shaped specimens, $5 \times 3 \times 14$ mm, fabricated from the powder mixture of diamond, Cu and B by SPS under a similar condition mentioned above. Coefficients of the thermal expansion, CTEs, of the composites were also investigated on square-column-shaped specimens, $5 \times 5 \times 14$ mm, fabricated from the powder mixture of diamond, Cu and B by SPS under a similar condition mentioned above. The thermal expansion of the composites was measured with a Rigaku TMA8310 dilatometer in a N2 flowing atmosphere with a heating ratio of 3 K/min in a temperature range between 243 and 483 K. The CTEs of the composites at room temperature were determined from the slope of the thermal expansion against temperature curve in a temperature range between 288 and 298 K.

3. Results and Discussion

3.1. Relative Packing Density of Composites Fabricated by SPS

The relative packing density of the diamond-particle-dispersed Cu-matrix composites fabricated was measured as a function of B content, which is shown in Figure 3. The packing density of Cu-diamond composite without B powder addition was 89.7%. On the other hand, the packing density of the composite increased with the addition of B and it was 93.2% - 95.8% at a B content range between 1.8 and 13.8 vol.% in Cu matrix. This increase of the packing density would be caused by some bimodal effect of B powder, which has a wide particle size distribution as shown in Figure 1. The packing density decreased monotonically with the addition of B at a B content range between 1.8 and 10.6 vol.% and then increased a little. However, the change in the relative packing density of Cu-diamond composite was only 2.6% at a B content range between 1.8 and 13.8 vol.% in Cu matrix. This result would by caused by no or negligible plastic deformation of B particles during SPS consolidation at 1173 K for 0.6 ks because of high melting point of B (Tm = 2349 K), much higher than that of Cu (Tm = 1356 K). The relative packing density obtained for (Cu-B)-50 vol.% diamond composites was
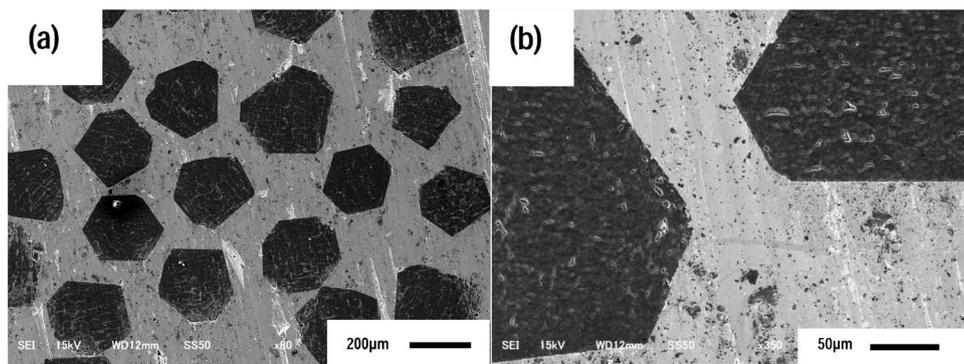
Figure 3. Schematic illustration showing processing of diamond particle dispersed Cu-matrix composite by spark plasma sintering (SPS).

93.2% - 95.8% in the present study, whereas that obtained for Al-50 vol.% diamond composite was higher than 99% in our previous work [30]. This lower packing density of (Cu-B)-diamond composites than that of Al-diamond composite is considered to take place because of different processing conditions. That is, (Cu-B)-diamond composite was fabricated in solid state during SPS, whereas Al-diamond composite was fabricated in continuous solid-liquid co-existent state. To increase the packing density of (Cu-B)-diamond composite, solid-liquid co-existent state processing would probably be effective with the addition of fourth element. In addition, processing at a much higher pressure as compared to that used in the present study would also be effective.
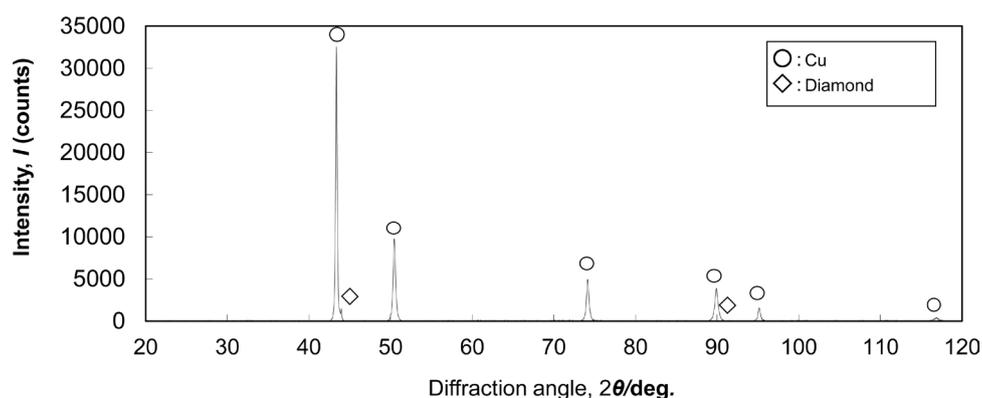
3.2. Microstructure

The microstructure of (Cu-7.2 vol.％B)-50 vol.% diamond composite sintered at 1173 K for 0.6 ks by SPS was investigated by scanning electron microscopy. **Figure 4** is scanning electron micrographs taken from a cross-section of (Cu-7.2 vol.％B)-50 vol.% diamond composite. As seen in **Figure 4(a)**, diamond particles are uniformly distributed in the composite without direct contact between diamond particles. No detection of the reaction phase on the interfacial boundary between the diamond particle and the Cu matrix was observed from SEM observation, as seen in **Figure 4(b)**. Many dark grey particles of 1 - 15 μm in diameter are observed in the Cu matrix. These particles are not precipitates but they are believed to be B particles in the powder mixture in the present study. It is because B addition of 7.2 vol.% into Cu powder is much higher than the solid-solubility limit of B (0.039 vol.%) in Cu. However, B particles in the Cu matrix could not be identified by SEM-EDX analysis. To identify B particles in Cu matrix, a detail analysis using EDS would be needed.

Figure 5 shows an X-ray diffraction pattern taken from (Cu-7.2 vol.%B)-50 vol.% diamond composite fabricated. Diffraction analyses revealed that two phases present in

Figure 4. Schematic illustration showing processing of diamond particle dispersed Cu-matrix composite by spark plasma sintering (SPS).
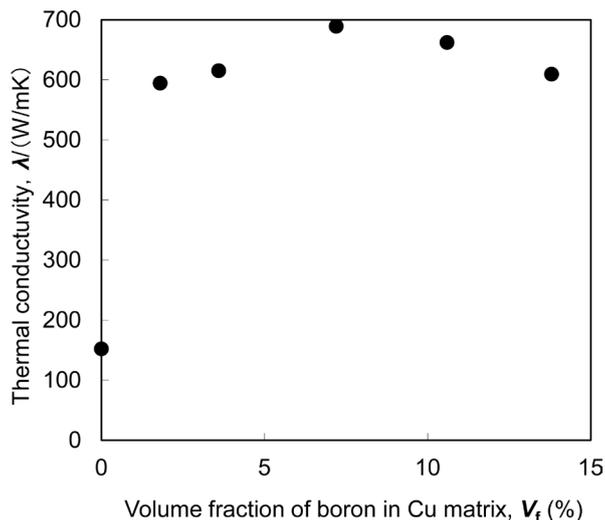

Figure 5. X-ray diffraction pattern taken from (Cu-7.2vol.%B)-50vol.%diamond composite fabricated by spark plasma sintering (SPS), showing two phases.
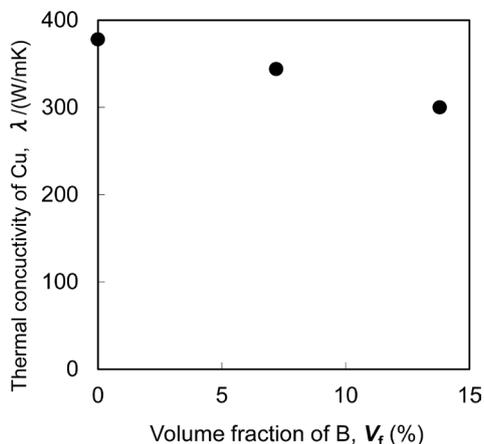
the composite were identified as Cu and diamond, and B phase was not identified. No detection of a peak from B by X-ray diffraction would be caused by the low content of B, 3.6 vol.% B (1.4 mass% B) in the composite, in addition to the low degree of crystallinity of B powder used in the present study.

3.3. Thermal Conductivity

Thermal conductivities of (Cu-B)-50 vol.% diamond composites fabricated by SPS were measured and the results obtained were plotted in Figure 6 as a function of the volume fraction of B in Cu matrix. As seen, the thermal conductivity of Cu-diamond composite without addition of B is only 152 W/mK, lower than that of pure-Cu, even although this composite contains 50 vol.% of diamond particles. The thermal conductivity of the composite, however, drastically increased with addition of B. The thermal conductivity obtained was 594 W/mK for (Cu-1.8 vol.% B)-50vol.% diamond composite. On the other hand, the thermal conductivity of (Cu-B)-diamond composite increased monotonically with increasing B content and the maximum thermal conductivity of 689 W/mK was obtained for (Cu-7.2 vol% B)-50 vol% diamond composite. Although the thermal conductivity of the composite slightly decrease with increasing B content at B content range between 7.2 and 13.8 vol.%, the thermal conductivity of 549 - 689 W/mK

Figure 6. Change in the thermal conductivity of (Cu-B)-50vol.% diamond composites fabricated by spark plasma sintering (SPS) as a function of the boron content in Cu matrix.

Figure 7. Change in the thermal conductivity of Cu consolidated by spark plasma sintering (SPS) as a function of the boron content.

was maintained at B content range between 1.8 and 13.8 vol.%.

To demonstrate the drastic increase of the thermal conductivity of Cu/diamond composites with addition of B, the powder mixtures composed of Cu and B were also consolidated at 1173 K for 0.6 ks by SPS and the change in the thermal conductivity of Cu with B addition was investigated. **Figure 7** shows changes in the thermal conductivity of Cu as a function of the volume fraction of B in Cu. As shown in **Figure 7**, the thermal conductivity of Cu monotonically decreases with increasing B content in Cu. Therefore, considering into account the results shown in **Figure 6** and those in **Figure 7**, the increase in the thermal conductivity of Cu/diamond composites with B addition would be caused by the improvement of bonding between diamond particles and Cu matrix.

Thermal conductivity has been evaluated for various materials including metal-matrix composites, polymer composites, ceramics and foods, using the following Hassel-
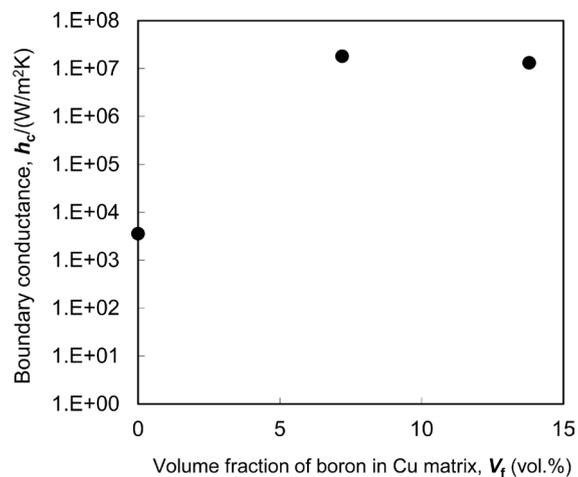
man-Johnson Equation (1) [31].

$$k = k_m \times \left(\frac{2\left(\dfrac{k_d}{k_m} - \dfrac{k_d}{ah_c} - 1\right)V_d + \dfrac{k_d}{k_m} + \dfrac{2k_d}{ah_c} + 2}{\left(1 - \dfrac{k_d}{k_m} + \dfrac{k_d}{ah_c}\right)V_d + \dfrac{k_d}{k_m} + \dfrac{2k_d}{ah_c} + 2} \right) \tag{1}$$

where, k is the thermal conductivity of the composite, k_d the thermal conductivity of dispersions (in this case, diamond, 2000 W/mK), k_m the thermal conductivity of the matrix (in this case, copper, 385 W/mK), V_d the volume fraction of dispersions, "a" the radius of dispersions (in this case, diamond, 155 μm) and h_c the boundary conductance.
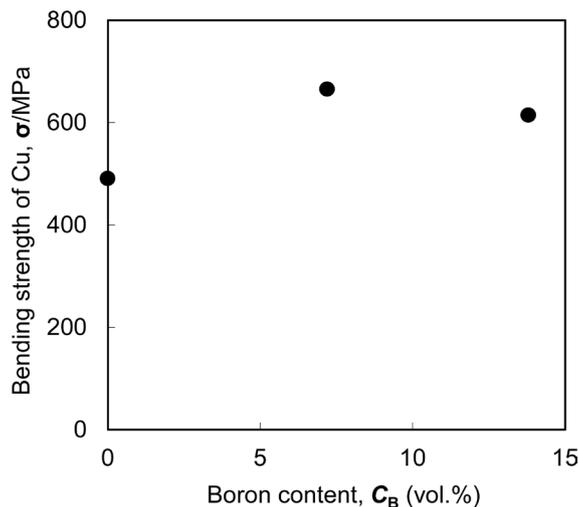
The boundary conductance h_c for the composite fabricated in the present work was calculated using Equation (1) and the results obtained are shown in Figure 8. The h_c value obtained for Cu-diamond composite without B addition was 3.59×10^3 W/m²K. h_c values, on the other hand, increased drastically with B addition and the h_c value of 1.80×10^7 W/m²K was for (Cu-7.2 vol.% B)-50 vol.% diamond composite and that of 1.31×10^7 W/m²K for (Cu-13.8 vol.% B)-50 vol.% diamond composite. In addition to the results shown in Figure 6 and Figure 7, the improvement of the bonding between Cu matrix and diamond particles with B addition will be shown by the result in Figure 8.
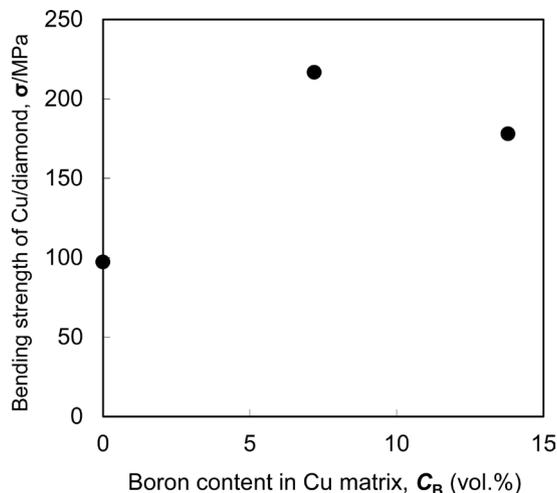
3.4. Mechanical Properties

The increase of h_c value of Cu/diamond composite with B addition was identified from resultant values using Hasselman-Johnson equation as described above. To carefully look at such an h_c value, it consists of two factors, the interfacial bonding and the quantity of porosities. Therefore, bending tests were carried out for Cu/diamond composites to clarify the effect of B addition for the bonding between diamond particles and Cu matrix in the composites. Change in the bending strength of Cu with B addition and that of Cu/diamond composite with B addition are shown in Figure 9 and Figure 10,

Figure 8. Change in the boundary conductance of (Cu-B)-50vol.% diamond composites as a function of the boron content in Cu matrix.

Figure 9. Change in the bending strength of Cu consolidated by spark plasma sintering (SPS) as a function of the boron content in Cu.

Figure 10. Change in the bending strength of (Cu-B)-50vol.% diamond composites fabricated by spark plasma sintering (SPS) as a function of the boron content in Cu matrix.
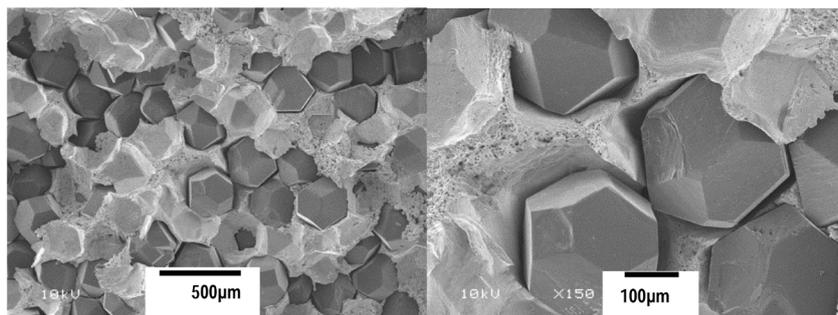
respectively. As seen in **Figure 9**, the bending strength of Cu without B addition is 491 MPa. However, the bending strengths of Cu-7.2 vol.%B and Cu-13.8 vol.%B are 666 and 615 MPa, which are 36% and 25% higher than that of Cu without B addition, respectively.

On the other hand, in the case of Cu-diamond composites, the bending strength of Cu-50 vol.% diamond composite is 97 MPa, as shown in **Figure 10**. This bending strength is very low in this case. By additions of B, however, drastic increase of the bending strength of Cu-diamond composite was attained. The bending strengths of (Cu-7.2 vol.%B)-50 vol.% diamond and (Cu-13.8 vol.%B)-50 vol.% diamond composites became 217 and 178 MPa, which were 123% and 83% higher than that of Cu-50 vol.% diamond composite without B addition, respectively. Considering into account the law of mixture for composite materials [32], the drastic increase of the bending
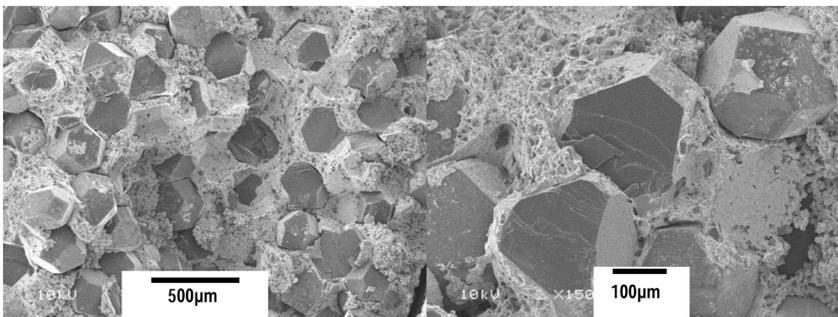
strength of Cu-diamond composite with B addition cannot be explained. The present drastic increase of the bending strength is considered to be caused by the improvement of bonding nature between diamond particles and Cu matrix.

Figure 11 shows bending fracture surfaces of diamond particle dispersed Cu matrix composites. In the case of Cu-diamond composite without B addition, all fractures occurred from the interfaces between diamond particles and Cu matrix, and many separations of diamond particles from Cu matrix were observed on the fracture surface of Cu-diamond composite. On the other hand, in the case of Cu-diamond composites with B addition, the bonding between diamond particles and Cu matrix is drastically improved and many transgranuler fractures of diamond particles were observed on the fracture surface of (Cu-B)-diamond composites. These results indicate the drastic im-
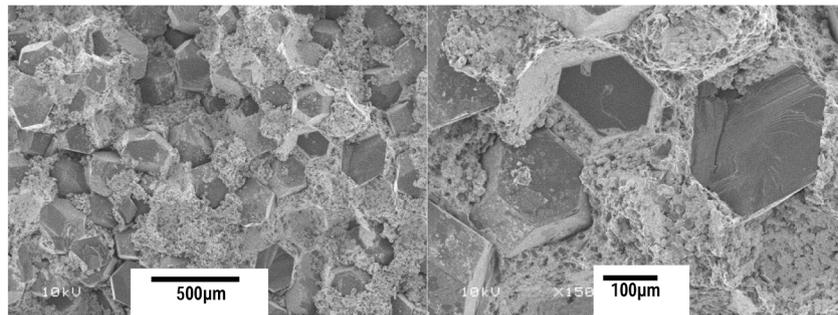
(a) Cu-50vol.%diamond

(b) (Cu-7.2vol.%B)-50vol.%diamond

(c) (Cu-13.8vol.%B)-50vol.%diamond

Figure 11. Bending fracture surfaces of diamond particle dispersed Cu matrix composites fabricated by spark plasma sintering (left: low magnification, right: high magnification). (a) Cu-50vol.% diamond composite, (b) (Cu-7.2 vol.%B)-50vol.% diamond composite and (c) (Cu-13.8 vol.%B) -50vol.% diamond composite.

provement of the bonding between diamond particles and Cu matrix with B addition. Although the improvement of the interfacial bonding between diamond particles and Cu matrix is considered to be the formation of boron carbides at the interface, the existence of boron carbides at the interface has not been identified at the present moment. Therefore, further detailed microstructure investigation is currently underway by using transmission electron microscopy.
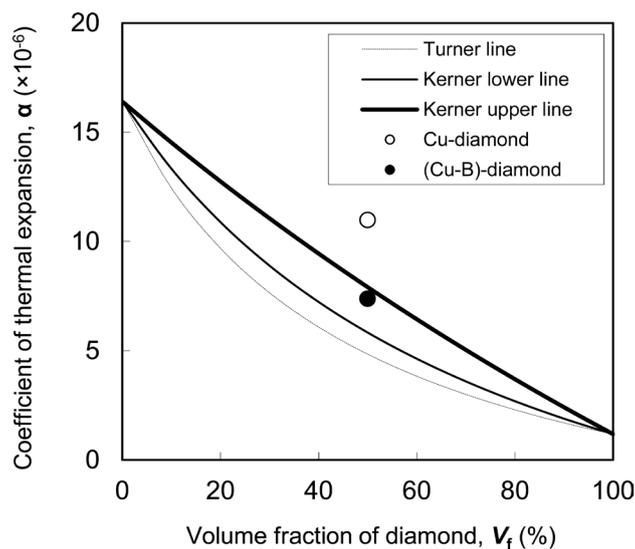
3.5. Coefficients of Thermal Expansion

Turner [33] and Kerner [34] have proposed models to theoretically calculate coefficients of the thermal expansion (CTEs) of composite materials. Kerner model takes account of shear effects at the boundaries between particles and their matrix, whereas Turner model takes no account of such effects. Consequently, Kerner model has widely been accepted for theoretical evaluations of the CTEs of composite materials. Hence, we also utilized Kerner model in the present study to evaluate the CTEs of the composites fabricated in the study. Kerner model is expressed by the following Equation (2),

$$\alpha_c = \alpha_m \cdot V_m + \alpha_d \cdot V_d + V_d V_m \left(\alpha_d - \alpha_m\right) \times \frac{K_d - K_m}{V_m K_m + V_d K_d + \left(3 K_d K_m / 4 G_m\right)} \tag{2}$$

where α_c is the CTE of the composite, α_d the CTE of the dispersions (which is 2.3×10^{-6}/K for diamond), α_m the CTE of the matrix (16.4×10^{-6}/K for Cu), V_d the volume fraction of the dispersions in the composites, V_m the volume fraction of the matrix in the composites, K_d the bulk modulus of the dispersions (44.2×10^{10} Pa for diamond), K_m the bulk modulus of the matrix (14.0×10^{10} Pa for Cu) and G_m the shear modulus of the matrix (4.6×10^{10} Pa for Cu and 47.8×10^{10} Pa for diamond).

Theoretically predicted and experimentally obtained CTEs for the diamond-particle-dispersed Cu-matrix composites were compared and the result is illustrated in **Figure 12**. Shown in this figure are the two lines obtained by reversing the role of matrix and dispersions in Kerner model. As seen, CTE obtained experimentally for Cu-50 vol.% diamond composite without B addition is 11.0×10^{-6}/K and much higher than the theoretical value estimated by the upper line of Kerner model, indicating the bonding between the diamond particle and the Cu matrix in the composite is very weak. On the other hand, CTE obtained experimentally for (Cu-7.2 vol.%B)-50 vol.% diamond composite is 7.4×10^{-6}/K and falls in the upper line of Kerner model. This is a good indication in that the diamond particles have bonded strongly with the Cu matrix in the composite fabricated by SPS in the present study. The decrease in CTE of Cu/diamond composite with B addition would be caused by the carbide formation at the interface between diamond particles and the Cu matrix via B particles. The CTEs of Cu-B/diamond composite obtained in the present study are 7.4×10^{-6}/K at 50 vol.% diamond. Considering into account $(4 \sim 8) \times 10^{-6}$/K of the CTEs for some packaging base materials currently in use, such as, Cu-W, Al/SiC and BeO, it is necessary to add more diamond powders to Cu-matrix composites, for example, as heat spreaders. That is, Cu-matrix-composites containing diamond higher than 50 vol.% would be preferable in application.

Figure 12. Comparison of coefficients of the thermal expansion predicted theoretically using Kerner model for Cu and Diamond composite and those obtained experimentally for Cu-50 vol. % diamond and (Cu-7.2 vol.%B)-50 vol.% diamond composite. Turner line obtained theoretically is also depicted.

4. Conclusion

Copper (Cu) matrix composites containing diamond particles were produced from the powder mixture composed of diamond, pure-Cu and boron (B) by spark plasma sintering. The microstructures were observed by scanning electron microscope (SEM) and the thermal properties were measured using a thermal constants analyzer and a dilatometer. The composites were consolidated at 1173 K for 600 s by SPS. The reaction between the diamond particle and the Cu matrix in the composite was not confirmed by SEM observation and X-ray diffraction (XRD) analysis. The relative packing density of the Cu/diamond composite increased with the addition of B and it was 93.2% - 95.8% at a B content range between 1.8 and 13.8 vol.% in Cu matrix. The thermal conductivity of the diamond particle dispersed Cu matrix composite increased with B addition and the maximum thermal conductivity of 689 W/mK was obtained for (Cu-7.2 vol% B)-50 vol% diamond composite. Numerous transgranular fractures of diamond particles were observed on the bending fracture surface of Cu/diamond composites with B addition. The coefficient of thermal expansion of the composite falls in the upper line of Kerner's model, indicating strong bonding between the diamond particle and the Cu matrix via B particles in the composite.

Acknowledgements

References

[1]   Halasz, G.S. (1995) Performance Trends in High-End Processors. *Proceedings of the IEEE*,

83, 20-36. http://dx.doi.org/10.1109/5.362754

[2] (1990) Properties and Selection: Nonferrous Alloys and Special-Purpose Mater. Metals Handbook, Vol. 2, 10th Edition, ASM Inter., 1119-1124.

[3] (1994) In: Bauccio, M., Ed., *ASM Engineered Mater.*, Reference Book, 2nd Edition, ASM Inter., Mater. Park, 360-369.

[4] Kerns, J.A., Colella, N.J., Makowiecki, D. and Davidson, H.L. (1995) Copper-Diamond Composite Substrates for Electronic Components. *Proceedings of* 28*th International Symposium on Microelectronics*, 28-37.

[5] Yoshida, K. and Morigami, H. (2004) Thermal Properties of Diamond/Copper Composite Material. *Microelectronics Reliability*, **44**, 303-308.
http://dx.doi.org/10.1016/S0026-2714(03)00215-4

[6] Mizuuchi, K., Inoue, K., Agari, Y., Yamada, S., Sugioka, M., Itami, M., Kawahara, M. and Makino, Y. (2007) Consolidation and Thermal Conductivity of Diamond Particle Dispersed Copper Matrix Composites Produced by Spark Plasma Sintering (SPS). *Journal of the Japan Institute of Metals*, **71**, 1066-1069. http://dx.doi.org/10.2320/jinstmet.71.1066

[7] Mizuuchi, K., Inoue, K., Agari, Y., Yamada, S., Tanaka, M., Sugioka, M., Takeuchi, T., Tani, J., Kawahara, M., Lee, J.-H. and Makino, Y. (2010) Thermal Properties of Diamond Particle-Dispersed Cu-Matrix-Composites Fabricated by Spark Plasma Sintering (SPS). *Materials Science Forum*, **638-642**, 2115-2120.
http://dx.doi.org/10.4028/www.scientific.net/MSF.638-642.2115

[8] Weber, L. and Tavangar, R. (2007) On the Influence of Active Element Content on the Thermal Conductivity and Thermal Expansion of Cu–X (X = Cr, B) Diamond Composites. *Scripta Materialia*, **57**, 988-991. http://dx.doi.org/10.1016/j.scriptamat.2007.08.007

[9] He, J., Wang, X., Zhang, Y., Zhao, Y. and Zhang, H. (2015) Thermal Conductivity of Cu-Zr/Diamond Composites Produced by High Temperature-High Pressure Method. *Composites Part B: Engineering*, **68**, 22-26.

[10] He, J., Zhang, H., Zhang, Y., Zhao, Y. and Wang, X. (2014) Effect of Boron Addition on Interface Microstructure and Thermal Conductivity of Cu/Diamond Composites Produced by High Temperature-High Pressure Method. *Physica Status Solidi A*, **211**, 587-594.
http://dx.doi.org/10.1002/pssa.201330237

[11] Fan, Y.-M., Guo, H., Xu, J., Chu, K., Zhu, X.-X. and Jia, C.-C. (2011) Effects of Boron on the Microstructure and Thermal Properties of Cu/Diamond Composites Prepared by Pressure Infiltration. *International Journal of Minerals, Metallurgy, and Materials*, **18**, 472-478.
http://dx.doi.org/10.1007/s12613-011-0465-2

[12] Chen, H., Jia, C.C. and Li, S.J. (2011) Effect of Cr Addition and Processing Conditions on Interface Microstructure and Thermal Conductivity of Diamond/Cu Co*mposite. Proceedings of the* 18*th International Conference on Composite Materials*, CD-ROM.

[13] Schubert, T., Trindade, B., Weißgärber, T. and Kieback, B. (2008) Interfacial Design of Cu-Based Composites Prepared by Powder Metallurgy for Heat Sink Applications. *Materials Science and Engineering: A*, **475**, 39-44. http://dx.doi.org/10.1016/j.msea.2006.12.146

[14] Schubert, T., Ciupinski, L., Zielinski, W., Michalski, A., Weißgärber, T. and Kieback, B. (2008) Interfacial Characterization of Cu/Diamond Composites Prepared by Powder Metallurgy for Heat Sinkapplications. *Scripta Materialia*, **58**, 263-266.
http://dx.doi.org/10.1016/j.scriptamat.2007.10.011

[15] Chu, K., Jia, C., Guo, H. and Li, W. (2013) Microstructure and Thermal Conductivity of Cu–B/Diamond Composites. *Journal of Composite Materials*, **47**, 2945-2953.
http://dx.doi.org/10.1177/0021998312460259

[16] Mankowski, P., Dominiak, A., Domanski, R., Kruszewski, M.J. and Ciupinski, L. (2014) Thermal Conductivity Enhancement of Copper-Diamond Composites by Sintering with Chromium Additive. *Journal of Thermal Analysis and Calorimetry*, **116**, 881-885. http://dx.doi.org/10.1007/s10973-013-3604-3

[17] Hall, H.T. (1960) Ultra-High-Pressure, High Temperature Apparutus: The "Belt". *Review of Scientific Instruments*, **31**, 125-131. http://dx.doi.org/10.1063/1.1716907

[18] Tamari, N., Tanaka, T., Tanaka, K., Kondo, I., Kawahara, M. and Tokita, M. (1995) Effect of Spark Plasma Sintering on Densification and Mechanical Properties of Silicon Carbide. *Journal of the Ceramic Society of Japan*, **103**, 12-17. http://dx.doi.org/10.2109/jcersj.103.740

[19] Fu, Z., Chen, W., Xiao, H., Zhou, L., Zhu, D. and Yang, S. (2013) Fabrication and Properties of Nanocrystalline $Co_{0.5}FeNiCrTi_{0.5}$ High Entropy Alloy by MA-SPS Technique. *Materials & Design*, **44**, 535-539. http://dx.doi.org/10.1016/j.matdes.2012.08.048

[20] Chen, H.S., Wang, W.X., Li, Y.L., Zhou, J., Nie, H.H. and Wu, Q.C. (2016) The Design, Microstructure and Mechanical Properties of B4C/6061Al Neutron Absorber Composites Fabricated by SPS. *Materials & Design*, **94**, 360-367. http://dx.doi.org/10.1016/j.matdes.2016.01.030

[21] Mizuuchi, K., Sugioka, M., Itami, M., Kawahara, M., Lee, J.H. and Inoue, K. (2003) Effects of Processing Condition on Properties of Ti-Aluminides Reinforced Ti Matrix Composites Synthesized by Pulsed Current Hot Pressing (PCHP). *Materials Science Forum*, **426-432**, 1757-1762. http://dx.doi.org/10.4028/www.scientific.net/MSF.426-432.1757

[22] Mizuuchi, K., Inoue, K., Sugioka, M., Itami, M. and Kawahara, M. (2004) Properties of *In-Situ* Ti-Aluminides Reinforced Ti Matrix Laminate Materials Synthesized by Pulsed Current Hot Pressing (PCHP). *Materials Transactions*, **45**, 249-256. http://dx.doi.org/10.2320/matertrans.45.249

[23] Mizuuchi, K., Inoue, K., Hamada, K., Sugioka, M., Itami, M., Fukusumi, M. and Kawahara, M. (2004) Processing of TiNi SMA Fiber Reinforced AZ31 Mg Alloy Matrix Composite by Pulsed Current Hot Pressing. *Materials Science and Engineering: A*, **367**, 343-349. http://dx.doi.org/10.1016/j.msea.2003.10.286

[24] Mizuuchi, K., Inoue, K., Sugioka, M., Itami, M., Lee, J. and Kawahara, M. (2006) Properties of Ni-Aluminides-Reinforced Ni-Matrix Laminates Synthesized by Pulsed-Current Hot Pressing. *Materials Science and Engineering: A*, **428**, 169-174. http://dx.doi.org/10.1016/j.msea.2006.04.113

[25] Mizuuchi, K., Inoue, K., Sugioka, M., Itami, M., Kawahara, M. and Yamauchi, Y. (2006) Microstructure and Mechanical Properties of Boron-Fiber-Reinforced Titanium-Matrix Composites Produced by Pulsed Current Hot Pressing (PCHP). *Materials Science and Engineering: A*, **428**, 175-179. http://dx.doi.org/10.1016/j.msea.2006.04.112

[26] Mizuuchi, K., Lee, J.H., Inoue, K., Sugioka, M., Itami, M. and Kawahara, M. (2008) High Speed Processing of Ni-Aluminides-Reinforced Ni-Matrix Composites by Pulsed-Current Hot Pressing (PCHP). *Journal of Modern Physics B*, **22**, 1672-1679. http://dx.doi.org/10.1142/S0217979208047249

[27] Mizuuchi, K., Inoue, K., Agari, Y., Kawahara, M., Makino, Y. and Ito, M. (2014) Thermal properties of Al/β-SiC Particle Dispersed Al-Matrix Composites Fabricated in Continuous Solid-Liquid Co-Existent State by SPS. *Journal of Metallurgical Engineering*, **3**, 59-68. http://dx.doi.org/10.14355/me.2014.0302.01

[28] Mizuuchi, K., Inoue, K., Agari, Y., Sugioka, M., Tanaka, M., Takeuchi, T., Tani, J., Kawahara, M., Makino, Y. and Ito, M. (2015) Bimodal and Monomodal Diamond Particle Effect on the Thermal Properties of Diamond-Particle-Dispersed Silver-Matrix Composite Fabricated by SPS. *Journal of Metallurgical Engineering*, **4**, 1-12.

http://dx.doi.org/10.14355/me.2015.04.001

[29] Mizuuchi, K., Inoue, K., Agari, Y., Sugioka, M., Tanaka, M., Takeuchi, T., Tani, J., Kawahara, M., Makino, Y. and Ito, M. (2016) Bimodal and Monomodalsic Particle Effect on the Thermal Properties of SiC Particle Dispersed Al-Matrix Composite Fabricated by SPS. *Journal of Metallurgical Engineering*, **5**, 1-12. http://dx.doi.org/10.14355/me.2016.05.001

[30] Mizuuchi, K., Inoue, K., Agari, Y., Morisada, Y., Sugioka, M., Tanaka, M., Takeuchi, T., Tani, J., Kawahara, M. and Makino, Y. (2011) Processing of Diamond Particle Dispersed Aluminum Matrix Composites in Continuous Solid-Liquid Co-Existent State by SPS and Their Thermal Properties. *Composites Part B: Engineering*, **42**, 825-831. http://dx.doi.org/10.1016/j.compositesb.2011.01.012

[31] Hasselman, D.P.H. and Jhonson, L.F. (1987) Effective Thermal Conductivity of Composites with Interfacial Thermal Barrier Resistance. *Journal of Composite Materials*, **21**, 508-5515. http://dx.doi.org/10.1177/002199838702100602

[32] Kelly, A. and Tyson, W.R. (1965) Fiber Strengthened Materials. In: Zackay, V.F., Ed., *High Strength Materials*, John Wiley & Sons Inc., New York, 578-583.

[33] Turner, P.S. (1946) Thermal Expansion Stresses in Reinforced Plastics. *NIST Journal of Research*, **37**, 239-250. http://dx.doi.org/10.6028/jres.037.015

[34] Kerner, E.H. (1956) The Elastic and Thermoelastic Properties of Composite Media. *Proceedings of the Physical Society Section B*, **69**, 808-813. http://dx.doi.org/10.1088/0370-1301/69/8/305